

**JURNAL SEGARA**
<http://ejournal-balitbang.kkp.go.id/index.php/segara>

ISSN : 1907-0659

e-ISSN : 2461-1166

Nomor Akreditasi: 766/AU3/P2MI-LIPI/10/2016

## HYDRODYNAMICS SABANG BAY AND ITS INFLUENCE ON NEAR-SHORE SEDIMENT TRANSPORT, WEH ISLAND, INDONESIA

## HIDRODINAMIKA TELUK SABANG AND PENGARUHNYA TERHADAP TRANSPORTASI SEDIMEN DEKAT PANTAI, PULAU WEH, INDONESIA

Ulung Jantama Wisna &amp; Ilham

<sup>1</sup>Research Institute for Coastal Resources and Vulnerability, Ministry of Marine Affairs and Fisheries, Republic of Indonesia  
Jl. Raya Padang-Painan KM 16, Bungus, Padang, West Sumatera 25245

Received: 10 May 2020; Revised: 19 August 2020; Accepted: 26 August 2020

**ABSTRACT**

Sabang Bay is one of the significant areas in Weh Island that becomes a center of marine tourism. Recently, massive urban development in coastal areas impacts on the increase of marine pollution and sedimentation issues within the bay. This study aimed to determine tidal current patterns and their influence on evoking sedimentation within the bay. An Acoustic Doppler Current Profiler (ADCP) was installed within the bay for 30 days, which recorded surface elevation, waves, and sea currents. The numerical hydrodynamic model was developed to figure tidal current features out, validated using field observation data. Sediment transport along the coast was determined by comparing the sediment transport and wave energy component in the form of flux equation. Tidal current speed ranging from 0-0.2 m/s moves predominantly southeastward and northwestward during flood and ebb tides, respectively. Significant wave height (Hs) ranges from 0.18-1 m with a period span of 3.5 seconds propagates toward within the bay, resulting in enhanced sedimentation within the gulf caused by the wave-induced scour and turbulence. Sediment budget transported within the bay reaches 1586.18 m<sup>3</sup>/year proving that the sediment movement remarkably occurs within the bay wherein the concentration of suspended sediment ranges from 5-35 mg/L and 2-25 mg/L during the high tidal and low tidal conditions, respectively. Scour and turbulence events induced by internal solitary waves generated from the Andaman Sea result in increased coarse-sized sediment deposition when the flood tide occurs. While, during ebb tide, the widespread distribution of suspended sediment will occur over the bay.

**Keywords:** Hydrodynamics, Sabang Bay, sediment transport, total suspended sediment.

**ABSTRAK**

Teluk Sabang merupakan salah satu kawasan penting di Pulau Weh yang menjadi pusat wisata bahari. Pembangunan besar-besaran di kawasan pesisir berdampak pada peningkatan polusi perairan dan masalah sedimentasi di dalam teluk. Penelitian ini bertujuan untuk mengetahui karakteristik hidrodinamika dan pengaruhnya terhadap peningkatan sedimentasi di dalam teluk. ADCP dipasang selama 30 hari pengukuran, yang merekam data elevasi permukaan, gelombang, dan arus laut. Model numerik hidrodinamika dikembangkan untuk menggambarkan kondisi arus pasang surut yang divalidasi menggunakan data pengamatan lapangan. Transpor sedimen sepanjang pantai diprediksi dengan membandingkan nilai transportasi sedimen dengan komponen energi gelombang dalam bentuk persamaan fluks. Arus pasang surut dengan kecepatan berkisar antara 0-0,11 m/s bergerak secara dominan masing-masing ke arah tenggara dan barat laut pada saat pasang dan surut. Tinggi gelombang signifikan (Hs) berkisar antara 0,2 – 1 meter dengan rentang priode 3.5 detik yang menjalar menuju dalam teluk sehingga peningkatan sedimentasi didalam teluk akibat gelombang yang membangkitkan gerusan dasar dan turbulensi sedimen. Asupan sedimen yang tertransportasi ke dalam teluk mencapai 1586,18 m<sup>3</sup>/tahun. Hal ini membuktikan bahwa pergerakan sedimen secara ekstrim terjadi di dalam teluk yang mana konsentrasi sedimen tersuspensi berkisar antara 5-35 mg/L dan 2-25 mg/L pada saat pasang dan surut. Gerusan dasar dan turbulensi sedimen dipengaruhi oleh gelombang internal tunggal yang terbentuk dari Laut Andaman yang akhirnya meningkatkan pengendapan sedimen berukuran kasar ketika pasang tinggi terjadi. Sedangkan saat surut, sebaran secara luas dari sedimen tersuspensi dapat terjadi di seluruh teluk.

**Kata kunci:** Hidrodinamika, Teluk Sabang, transpor sedimen, total sedimen tersuspensi.

Corresponding author:

Jl. Pasir Putih I Ancol Timur, Jakarta Utara 14430. Email: [ulungjantama@gmail.com](mailto:ulungjantama@gmail.com)

Copyright © 2019 Jurnal Segara

DOI: <http://dx.doi.org/10.15578/segara.v16i2.8980>

## INTRODUCTION

Sedimentation issues have become a significant problem that occurred in most bays in Indonesia (Wisha *et al.*, 2019). A weak circulation of water mass in the semi-enclosed water area is predicted as a triggering factor. Massive developments frequently applied in coastal areas have a role in inducing coastline instability (Fantinato, 2019). On the other hand, sedimentation will impact higher suspended sediment-induced turbidity (Andutta *et al.*, 2019). If ongoing, this condition may deteriorate biota survival ability and induce pollution.

High degradation of coastline areas was reported by the local community several years ago in Sabang Bay. It is located in the northern Weh Island, Aceh Province. As the center of marine tourism, Sabang Bay has become the area of significance where many tourist attractions exist, such as Sophie Rickmers shipwreck diving site, the hot bubble (seafloor fumaroles), etc. (Gemilang & Wisna, 2019). Due to its potentials, development in the coastal area along Sabang Bay has been constructed in the form of resorts, connecting roads, souvenir stores, etc. which resulted in some new problems such as the increase of debris, social-economic issues, pollution, and higher sedimentation within the bay.

The high sedimentation in Sabang Bay sufficiently got worse (Wisha *et al.*, 2019). The dynamic of water flow and sediment characteristics are predicted as the main factors triggering this issue. Massive developments of hard structure in the coastal area of Sabang has a significant impact on coastal instability (Ondara *et al.*, 2019). Furthermore, the constructions contribute to the increase of sediment waste into the waters (Agus, 2019), instantly increasing turbidity and suspended sediment within the bay. With time, the accumulation of anthropogenic sediment will elevate and affect the ecosystem and water quality degradation.

Natural factors such as waves, currents, and tides have a unique role in transport mechanism within Sabang Bay whereby the extreme atmosphere-ocean interactions occurred in the Indian Ocean gives an extraordinary impact on abrasion and sedimentation along the coastline (Setiawan *et al.*, 2018). At certain times, the wind-wave-driven current brought high sediment intake toward the Bay so that exogenic sediment took place in inducing high resuspension (Purnawan *et al.*, 2018), supported by the anthropogenic sediment, and the more elevated sedimentation will endanger Sabang Bay (Purnawan *et al.*, 2016). As a semi-enclosed water area, the tidal-current regime is predominant to control the reverse oscillation of water masses within the bay which the low transport mechanism takes place due to many existing obstacles

within the bay such as the geomorphological and topographical features which hamper the movement of water mass and induce some deformations of the current flow (Bayhaqi *et al.*, 2018; Wisna *et al.*, 2015). Due to the influence of oceanography-related aspects, this study will determine hydro-oceanography characteristics and their impact on the transport of sediment within Sabang Bay.

Several previous related studies have been published that determine the oceanography profiles in Sabang Bay such as Gemilang & Wisna (2019) defined the influence of surface current on the distribution of surface temperature evoked by seafloor fumaroles, while Wisna *et al.* (2019) and Ondara *et al.* (2019) assessed the feasibility of offshore aquaculture based on the hydro-oceanography data. Nevertheless, the sedimentation issue is rarely studied in Sabang Bay. The sedimentation events frequently led the bay's water degradation and threatened the existence of several tourism objects beneath the waters. Thus, a study evaluating suspended sediment behavior is essential. This study aimed to determine the wind-wave-induced current and its role in triggering sediment transport and turbulence within Sabang Bay.

## METHODOLOGY

### Study Area and Hydrodynamic Model Set-up

A field survey was conducted on March, 16<sup>th</sup> 2017, within Sabang Bay. Three mooring stations were chosen to represent east, west, and south parts within Sabang Bay. Acoustic Doppler Current Profiler (ADCP)-Nortek was installed continuously at those three stations. Moreover, water was sampled for examining Total Suspended Sediment (TSS). The survey location, ADCP positions, and TSS observation points are shown in Figure 1. ADCP will record some parameters such as waves, currents, and tides. Those data will be used to validate the model results so that the model developed can adequately depict the real condition in the field (Chen *et al.*, 2015). The model result examination was performed by employing root mean square error (RMSE) formula as follow:

$$RMSE = \sqrt{\frac{1}{n} \sum_{i=1}^n (y - y_i)^2} \dots\dots\dots (1)$$

where:  
 n = total data that will be verified  
 y = model result data  
 yi= field measurement data

Tidal current patterns were modeled using flow model flexible mesh (fm) generated by considering coastline digitation, bathymetry, and tidal forecast as

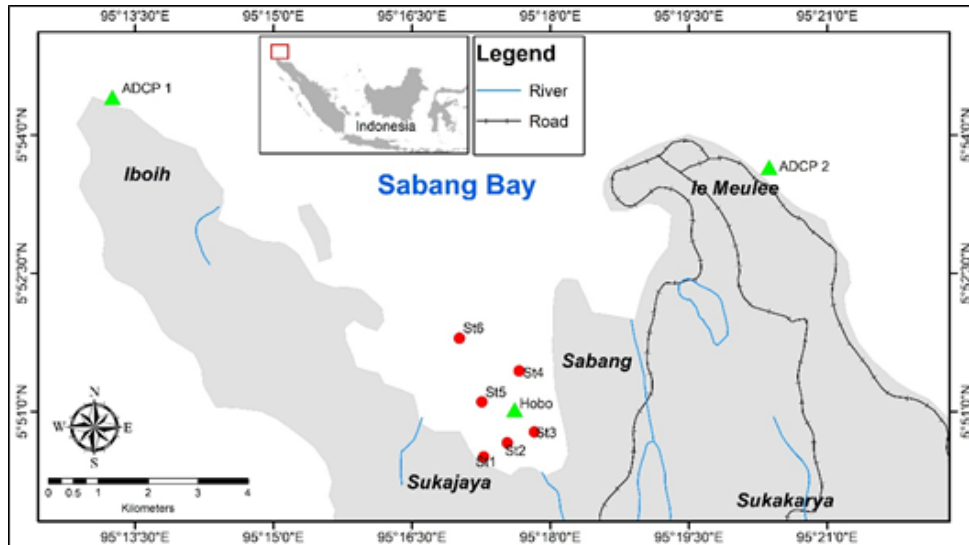


Figure 1. Research Location Map.

the model input. The model set-up is shown in Table 1. Model results will be mapped according to the four tidal extreme conditions (the spring and neap tidal conditions). The development of flow model fm was based on the discretization of continuity (2) and momentum equations for x component (3) and y component (4) (Bayhaqi *et al.*, 2018) as follows:

$$\frac{\partial u}{\partial x} + \frac{\partial v}{\partial y} + \frac{\partial w}{\partial z} = S \quad \dots\dots\dots 2)$$

$$\frac{\partial u}{\partial t} + \frac{\partial u^2}{\partial x} + \frac{\partial vu}{\partial y} + \frac{\partial wu}{\partial z} = fv - g \frac{\partial \eta}{\partial x} - \frac{1}{\rho_o} \frac{\partial p_a}{\partial x} - \frac{g}{\rho_o} \int_z^\eta \frac{\partial \rho}{\partial x} dz - \frac{1}{\rho_o h} \left( \frac{\partial s_{xx}}{\partial x} + \frac{\partial s_{xy}}{\partial y} \right) + F_u + \frac{\partial}{\partial z} \left( v_t \frac{\partial u}{\partial z} \right) + u_s S \quad (3)$$

$$\frac{\partial v}{\partial t} + \frac{\partial v^2}{\partial y} + \frac{\partial uv}{\partial x} + \frac{\partial wv}{\partial z} = -fv - g \frac{\partial \eta}{\partial y} - \frac{1}{\rho_o} \frac{\partial p_a}{\partial y} - \frac{g}{\rho_o} \int_z^\eta \frac{\partial \rho}{\partial y} dz - \frac{1}{\rho_o h} \left( \frac{\partial s_{yx}}{\partial x} + \frac{\partial s_{yy}}{\partial y} \right) + F_v + \frac{\partial}{\partial z} \left( v_t \frac{\partial v}{\partial z} \right) + v_s S \quad (4)$$

where:

- t = unit of time
- x,y,z = the component position in the cartesian coordinates
- η = elevation changes
- d = still water depth (h=η+d -->total water depth)
- u,v,w = velocity components in the x, y and z directions
- f = Coriolis force
- g = specific gravity
- ρ = water density
- s<sub>xx</sub>, s<sub>xy</sub>, s<sub>yx</sub>, s<sub>yy</sub> = radiation stress tensor components
- v<sub>t</sub> = Eddy viscosity
- p<sub>a</sub> = atmospheric pressure
- ρ<sub>o</sub> = reference density for water
- S = magnitude of discharge according to point sources
- (u<sub>s</sub>, v<sub>s</sub>) = velocity components (the water is discharged into the ambient water)

**Sediment Transport Estimation**

Sediment transport within Sabang Bay was estimated from an empirical equation developed based on field survey data retrieval. In this stage, the wave energy flux component was predicted in the form of flux equation (Triatmodjo, 2012) as follow:

$$P_1 = \frac{\rho g}{8} H_b^2 C_b \sin \alpha_b \cos \alpha_b \quad \dots\dots\dots (5)$$

where:

- P<sub>1</sub> = wave energy flux component along the coast at the time of breaking (kg.m/d)
- ρ = specific gravity of sea water (kg/m<sup>3</sup>)
- g = acceleration of gravity = 9.81 (m/s<sup>2</sup>)
- H<sub>b</sub> = breaking wave height (m)
- C<sub>b</sub> = breaking wave celerity (m/s)=√(gd<sub>b</sub>)
- α<sub>b</sub> = breaking wave angle

To predict total transport annually, we employed a formula developed by Triatmodjo (2012). The scenario was applied to the vast area in the surf zone, where sediment transport is difficult to determine. In this model, the bed sediment characteristics were not considered so that we only applied this model for homogenous sediment, in which the diameter of each particle ranged from 0.175-1 mm. The sediment budget prediction is developed by executing a formula as follow:

$$Q_s = \frac{K}{(\rho_s - \rho)g(1 - n)} P_1 \quad \dots\dots\dots (6)$$

where:

- Q<sub>s</sub> = sediment budget along the coast (m<sup>3</sup>/s)
- K = Given by CERC (1984), K=0.39, in which the formula above used significant wave height value

Table 1. Flow model fm set-up

Parameter	Implemented in the simulation
Time of simulation	Number of time step = 100 Time step interval = 600 sec Simulation start date = 16/03/2017 19:00 Simulation end date = 31/03/2017 19:00
Mesh boundary	SRTM bathymetry data combined with field survey result Google Earth coastline digitation
Flood and dry	Drying depth = 0.005 m Flooding depth = 0.05 m Wetting depth = 0.1 m
Boundary conditions	Type = Specified level Format = Varying in time, constant along boundary Time Series = Tide forecasting with coordinates below: 1. Longitude: 95,299, Latitude: 5,934 2. Longitude: 95,400, Latitude: 5,836 3. Longitude: 95,299, Latitude: 5,739 4. Longitude: 95,199, Latitude: 5,836

$\rho_s$  = Specific gravity of sand (kg/m<sup>3</sup>)  
 $n$  = Porosity (n≈0.4)

**Suspended Sediment Model Development**

Sediment transport in the form of the suspended particle was calculated by considering bedload and suspended load so that the model developed could predict sediment mass separately, which was then tabulated to gain sediment mass in total according to its mass concentration. The concentration of total suspended sediment is based on Eddy viscosity and settling velocity as follow:

$$\frac{\partial C_i}{\partial t} + \frac{\partial u C_i}{\partial x} + \frac{\partial v C_i}{\partial y} + \frac{\partial (w - w_i) C_i}{\partial z} = \frac{\partial (A_u \frac{\partial C_i}{\partial x})}{\partial x} + \frac{\partial (A_u \frac{\partial C_i}{\partial y})}{\partial y} + \frac{\partial (K_h \frac{\partial C_i}{\partial z})}{\partial z} \quad (7)$$

where:

- $C_i$  = Concentration value of suspended sediment
- $A_u$  = Horizontal Eddy viscosity
- $K_h$  = Vertical Eddy viscosity
- $w - w_i$  = Settling velocity adjusted with sediment type applied in the model

The vertical Eddy viscosity is adjusted according to depth layer which in the surface layer, the value of flux boundary condition used  $K_h \frac{\partial C_i}{\partial z} = 0, z = \zeta$ , for the surface bottom layer, the vertical Eddy viscosity is distinguished considering deposition and erosion events whereby the Eddy viscosity formula is given  $K_h \frac{\partial C_i}{\partial z} = \Delta t Q_i (1 - P_b) F_{bi} (\frac{\tau_b}{\tau_{ci}} - 1) - D_i, z = \zeta$  where  $Q_i$  is erosion flux,  $P_b$  is porosity in the surface bottom,  $F_{bi}$  is sediment fraction,  $\tau_b$  is bottom shear stress, and  $\tau_{ci}$  is critical shear stress of sediment. The results were validated using TSS concentration from field measurement conducted by (Tanto *et al.*, 2018).

**RESULTS AND DISCUSSION**

**Hydrodynamic Characteristics**

Table 2 shows the tidal constituent analyzed using the Least Square method. Overall, the semidiurnal components of tidal show a strong predomination, mainly for M2 and S2 constituent. This condition indicates that in Sabang Bay, the tidal type is semidiurnal proven by the Formzahl of 0.12 (semidiurnal tides). Thus, for

Table 1. Flow model fm set-up

Constituent	Amplitude (cm)	Phase delay (°)
M2	44.61	50.88
S2	71.12	21.98
N2	9.15	87.71
K2	56.85	225.00
K1	10.87	230.55
O1	3.64	143.93
P1	5.00	105.90
M4	1.10	148.33
MS4	1.77	102.79
SO	1140.38	MSL

almost 24 hours, there are two nearly equal high tidal and low tidal conditions. While the tidal type defines from the differences of amplitude, cycles in tidal range (height difference between consecutive flood and ebb elevation) depend on differences in phase delay (Boon, 2013; Van Rijn, 2011).

Due to the phase delay difference between M2 and S2, M2 is going to complete each 360o cycle a very sooner because it will complete around 51o in an hour while S2 completes around 22o. Table 1 shows diurnal constituents such as K1, O1, and P1 tend to be weak with a quite rapid phase delay reaching 230°, 144°, and 105°, respectively. Moreover, the N2 constituent shows a uncertain magnitude among the semidiurnal constituents. It indicates that the maximum range of tidal did not exist during the record of tidal data. This maximum range will happen when M2, S2, and N2 are in the peak magnitude at about the same time, and it is called perigean-spring tides of the maximal range that occur several times a year (Menéndez & Woodworth, 2010).

Except for S0 value, the last two constituents (M4 and MS4) are called shallow-water tides. Tides propagating waters where the tidal range is no longer insignificant compared to the water depth experience a deformation that produces new waves (overtides) additionally. A compound tide (MS4) arises in shallow water resulted from the interaction between its two parent waves (M2 and S2) in shallow water. These constituents will have a role in reconstructing the tidal asymmetries and other fine-scaled behaviors (Andutta *et al.*, 2019). Furthermore, the MSL observed is 1.14 meters.

According to a 20-year prediction, the significant elevation of tidal in Sabang Bay is shown in Figure 2. The maximum water level during spring conditions is 1.95 meters above MSL. In contrast, the average maximum surface level is 1.41 meters, with the highest

elevation of 0.92 meters above MSL. On the other hand, during 20-year tidal prediction, we also identified the lowest water level during spring tidal conditions of 1.86 meters beneath MSL, while, the average minimum surface level during spring tidal conditions is 1.34 meters, with the lowest value of 0.91 meters beneath MSL. The variability of surface elevation changes has a role in generating surface currents and transport mechanisms in the estuarine area (Chen & de Swart, 2018). The higher the elevation formed, the more substantial transport energy resulted from this tidal fluctuation (Qarnain *et al.*, 2014).

Through the velocity component of current data acquisition, we proved that the tidal current is a predominant inducing transport mechanism within Sabang Bay. It is shown by the elliptical formations of a scatter plot in each layer of the water column (Stanton *et al.*, 2001) shown in Figure 3 and Figure 4. At station ADCP 1, the current velocity in the surface ranges from -0.4 up 0.8 m/s. The surface current seems more erratically in which the zonal velocity of current shows a relatively positive value meaning that the horizontal transport takes place with eastward directions. The more deeply the water column, the lower velocity of the current, in the 5-7 meters depth, the profile of sea currents ranging from -0.4 up to 0.6 m/s seems more stable, whereby the influence of wind-driven current gradually declines. In contrast, in the surface bottom, the velocity of current becomes weaker ranging from -0.3-0.4 m/s caused by the many factors such as bottom friction, the higher value of density, and some other forces (Van Rijn, 2011). If we see in more detail, the tidal ellipses that rotate counterclockwise bottomward show the influence of Coriolis forces (Chen & de Swart, 2018). This event also determines that the Ekman spiral principal controls the vertical transport that occurred in Sabang Bay.

At station ADCP 2, the depth is shallower than the first station of ADCP. It is only 7.5 meters in depth

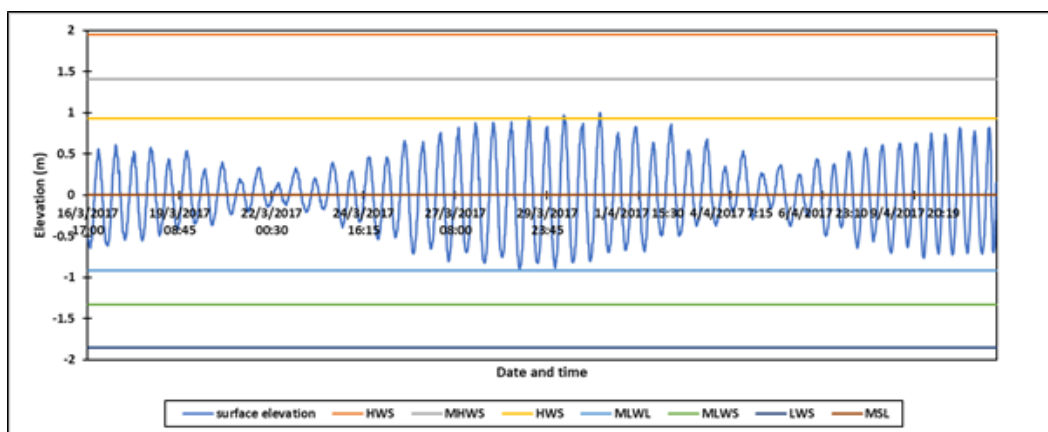


Figure 2. Significant elevation of tidal within Sabang Bay.

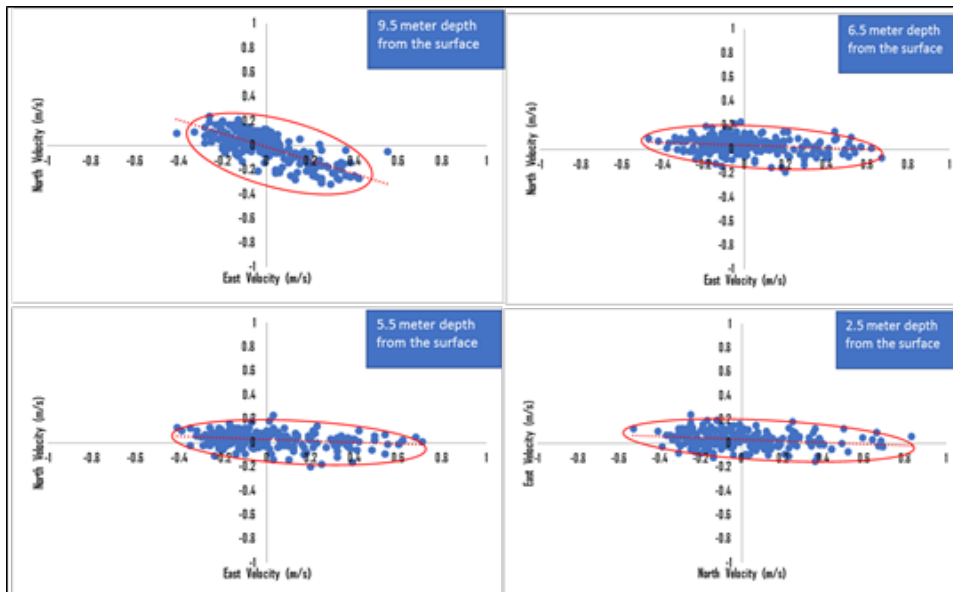


Figure 3. Velocity component of current profile at Station ADCP 1.

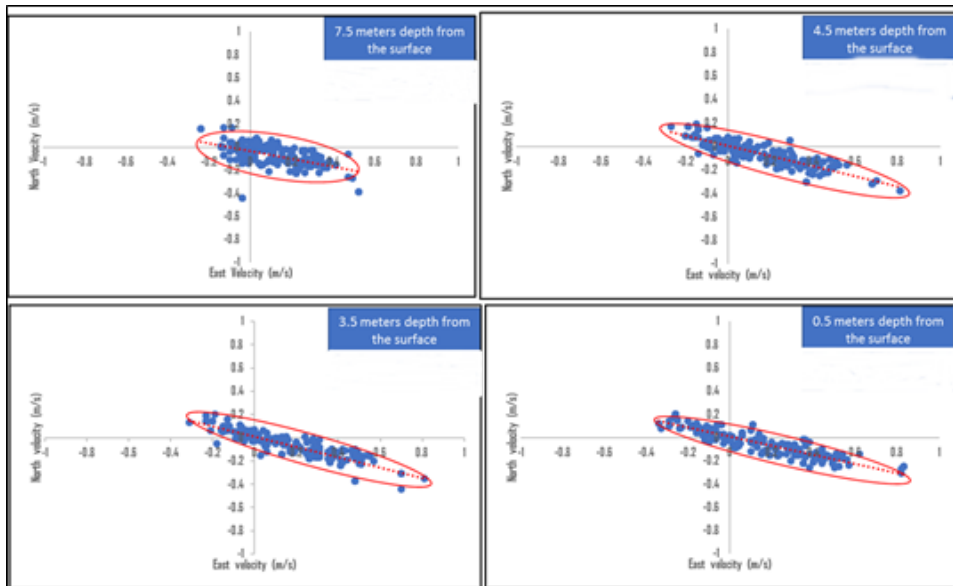


Figure 4. Velocity component of current profile at Station ADCP 2.

recorded. Unlike the other stations, the Ekman spiral could not be determined due to the shallow water area. Moreover, from the surface water to the 4.5 meters beneath the surface, the current velocity shows a stable speed, ranging from -0.3 up to 0.6 m/s, illustrating that the influence of wind-driven current takes place until the depth of around 5 meters underneath the surface. In contrast, in the surface bottom, the velocity dramatically decreases, ranging from -0.1 to 0.4 m/s. This condition proves that the working forces in the shallow waters are stronger in hampering the vertical and horizontal water mass movements. Regarding the shallow-water tides, the strong amalgamation of M2-S2 tidal constituent will result in tidal asymmetry whereby this event can be the most definite obstacle to water

mass movement in shallow waters (Hunt *et al.*, 2015).

Figure 5 illustrates the wave features within Sabang Bay. Overall, the value of significant wave height ( $H_s$ ) is inversely proportional to its period ( $T_s$ ). While, during wave measurement, the northerly wave was taking place propagating toward the south within the bay. The  $H_s$  value ranges from 0.18 – 1.1 meters, with a period span of 3.5 seconds. The higher the breaking wave formed, the longer the period to reach one wavelength. This correlation is proven by the R square value of 0.89, which means that between those variables were influencing each other with around 89 percent of the relationship. The more extended period observed in reaching one wavelength is caused by the

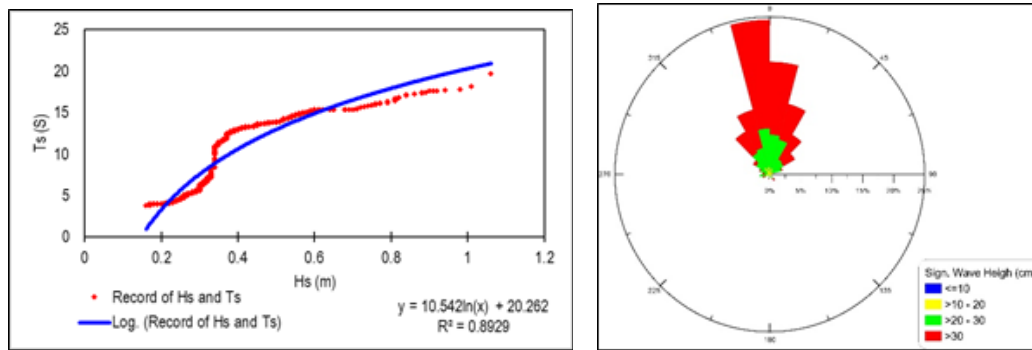


Figure 5. Records of ocean wave profile within Sabang Bay.

significant depth changes and deceleration of wave group velocity (Ondara *et al.*, 2018). Regarding the dominant wave direction, almost 90 percent of wave directions (Hs between 1-3 meters) move from the north toward the south. This condition indicates that the influence of solitary waves from the Andaman Sea and Bengal Bay on triggering shallow-water waves is quite strong. According to Rachmat & Purwanto (2016), the breaking wave after passing the swell area transforms longshore currents, which have a role in triggering sediment transport near the coast. It is believed that the intensive and robust influence of waves will form a stronger longshore current, contributing to the local sediment transport within Sabang Bay.

**Tidal Current Pattern**

Before we use the result of model simulation to depict field conditions, initiating the model validation stage is essential to measure the error resulted from the model developed. Model development is an approachable way to illustrate natural conditions. In this stage, we compared the surface elevation data to examine how much the error value resulted from the flow model development by applying sea surface elevation data (Figure 6). The comparison was performed by more than 15 days of tidal data representing neap and spring phases. Overall, throughout examined data, a similar period with a slight differential in elevation was observed whereby the elevations of field measurement data were higher with around 0.1-0.2 meters than the

model data.

The RMSE was 7.83 %, proving that the simulated model results can be used for further analysis. According to (Gemilang *et al.*, 2020), the error of a developed model can be accepted to represent the field condition if it is not more than 15 %. If we see in more detail, even though during spring tidal conditions, the deviation of the symmetrical tidal phase is higher, but during neap tidal conditions, the surface depiction is likely to reflect an erratic fluctuation probably caused by the influence of waves. According to Ondara *et al.* (2018), the generation of waves is almost simultaneously with tidal elevation displacement. That is why the formation of surface water tends to have a sharp fluctuation due to wind-wave-driven surface current influences.

Figure 7 shows tidal current patterns during the four extreme tidal conditions. Generally, the tidal-current trends during spring and neap tidal conditions are not different, whereby the dominant direction is almost the same between flood and ebb tide. The current magnitude ranges from 0-2 m/s and 0-1.89 m/s during spring and neap tidal conditions. During the spring phase, the tidal current showed a sufficiently strong feature of water mass movement.

At the high spring tidal condition, the current speed within Sabang Bay ranged from 1.14-2 m/s (Figure 7A). The water mass moved toward within the bay because,

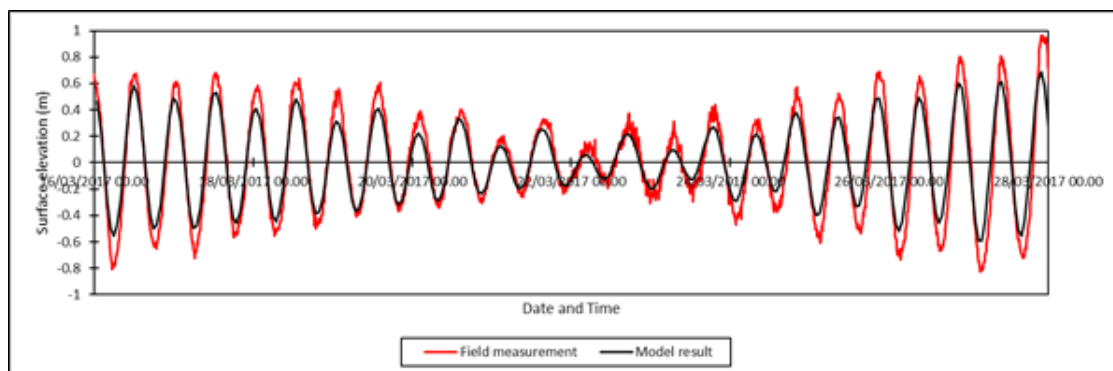


Figure 6. Records of ocean wave profile within Sabang Bay.

during this phase, the elevation of seawater was higher than the shore elevation, so that the water mass flowed toward the lower pressure area. Northerly and easterly sea currents commenced entering the bay, which possibly brought coarse sediments from the sea provenance. According to Gemilang *et al.* (2020), the relatively coarse sea-sourced sediments will potentially be transported by reliable energy of currents by which the residue will be settled in the deposition environment near the coast in which the sea-current features tend to be weak.

Asymmetrical currents are observed in the southern Rubiah, and Klah Island, wherein the current direction is oppositely formed. This event is caused by the deformation of the solitary wave from the Andaman Sea while passing a narrowed area between small islands. The current speed becomes faster with a possibly asymmetrical direction, called a diffraction event (Tsai *et al.*, 2001).

After reaching the peak flood tide, the water level started to decrease with a briefly slack water event during that displacement process (Blanton *et al.*, 2002). The opposite direction of the current was identified during the low spring tidal condition with speed ranging from 0.05-1.47 m/s (Figure 7B). In the semi-enclosed bay, the water mass movement is like a “see saw”

whereby during this lowest phase of water level, the sea elevation is more moderate than shore area, so that the water mass moved sea-ward.

During neap tidal conditions, the sea-current feature was weaker than the spring conditions because the astronomical forces that perpendicularly positioned, resulting in the weakened energy-generated tides (Qarnain *et al.*, 2014). At the flood tides (Figure 7C), the current speed ranged from 0.15-1.89 m/s with a relatively southeastward direction. In contrast, at the low neap tidal condition (Figure 7D), the current flow was the weakest at all, ranging from 0.01-0.15 m/s with a relatively northwestward direction.

If we compare the spring and neap phases of tidal, it is predicted that the sediment transport will mostly take place during spring conditions, whereby the current features are pretty much more reliable than the neap one. The coarse sediments will be transported toward the coast during flood tides, which tends to be settled due to its more significant mass (Gemilang *et al.*, 2020). Otherwise, the finer-sized sediment sourced from river and land will be dominating the coastal area during ebb tides (Gemilang *et al.*, 2018), which triggers resuspension resulting in the higher suspended sediment within Sabang Bay (Gemilang & Wisna, 2019).

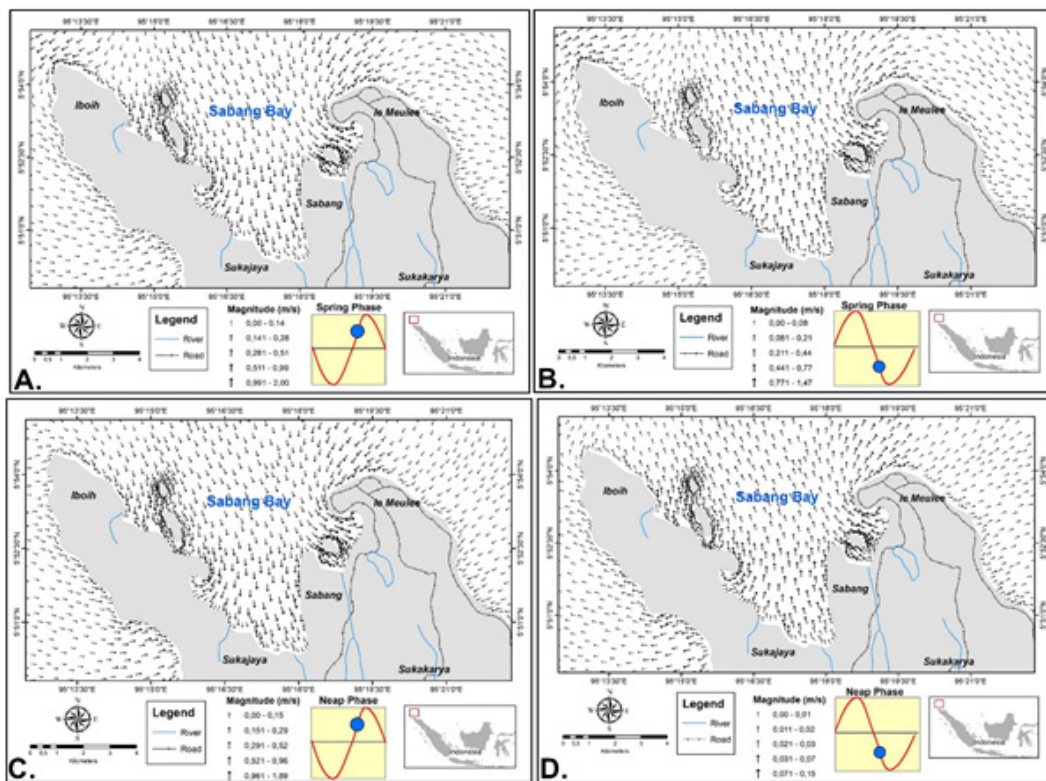


Figure 7. Tidal current patterns around Weh Island; A. during the high spring tidal condition; B. during the low spring tidal condition; C. during the high neap tidal condition; D. during the low neap tidal condition.



**Sediment Transport Prediction and TSS distribution**

Moving forward after the flow model simulation run, we developed the hydrodynamic model to predict the total sediment transport along the coast of Sabang Bay. This model is a one-line model so that the estimated sediment transport will be divided into two directions: right-ward and left-ward transport. Overall, the sediment transport is in line with tidal current features at each extreme tidal condition (Figure 9). The right-ward transport is higher during flood tides, while it is lower during ebb tides and vice versa for the left-ward transport.

The highest sediment transport was identified mostly during high tidal conditions with more than 12 m<sup>3</sup>/day in total. While during low tidal conditions, the total sediment transport was less than 8 m<sup>3</sup>/day. Total transport of sediment is the tabulation of rightward and left-ward transport at each tidal condition. If we accumulate, it is assumed that within a week, the total sediment transport reaches 84 m<sup>3</sup>/week. Moreover, the total annual transport resulted from the model was 1586.18 m<sup>3</sup>/year. For the semi-enclosed water area, those values are quite significant in terms of sediment transport. The influence of water mass transfer from the Indian Ocean, Andaman Sea, and Malacca Strait on inducing a great wave propagating Sabang Bay frequently takes place (Schott *et al.*, 2009). It is proven by the wave data (see in Figure 5) that the significant wave height was reaching 1 meter at certain times. According to Kench & Mclean (2004), the higher the wave height propagating costal-ward, the higher volume of sediment transport, which during its propagation, the wave particle's circle orbital will induce a dramatic scour and turbulence in the surface bottom (Wisha *et al.*, 2017). To conclude, the amalgamation of oceanography factors influence has a significant role in

inducing sediment transport near the coast of Sabang Bay.

As mentioned above, sediment transport's prediction was developed from waves and currents data, whereby it is the main factor generating scour and turbulence along the coastline. To determine the scour and turbulence events, we modeled the distribution of total suspended sediment (TSS) shown in Figure 9. This model was validated using the TSS concentration observed in the field. The defined RMSE was 11.86 %.

At the high spring tidal condition, the TSS concentration ranged from 5-30 mg/L. The higher level of TSS was identified in the area near the coastline (Figure 9A) with around 20-30 mg/L. The distribution of TSS was concentrated along the coast because of the propulsive force of tidal current (see in Figure 7A). The current direction heading toward within the bay pushed the water mass carrying sea-sourced sediment toward the closest plateau so that the accumulation of sediment will be relatively land-ward. The sea-sourced sediment, usually a coarse-sized particle, tends to be settled (Gemilang *et al.*, 2020). On the other hand, the river-sourced fine sediment will be suspended in the water column and surface. With the forceful current profile, the higher suspended sediment will be retained due to the intensive scour and turbulence events.

Unlike the flood tide at the spring phase, the distribution of suspended sediment was more widespread at the low spring tidal condition (Figure 9B). The TSS concentration ranged from 5-35 mg/L. The river-sourced sediment with fine-sized particles dominated the Sabang Bay. If we refer to Figure 8, the sediment transport is lower than the flood tide phase; however, during the ebb tide phase, the suspended

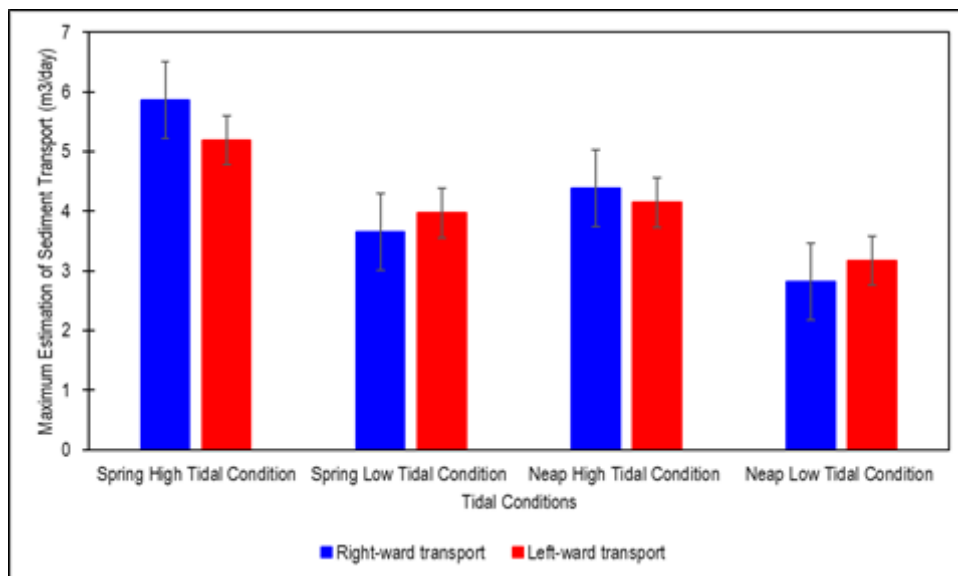


Figure 8. Maximum estimation of sediment transport within Sabang bay according to tidal conditions.

sediment concentration was higher than the flood tide one. As mentioned before that during low tidal conditions, the sea elevation was lower inducing seaward water mass movement so that the river intake of sediment will be widely distributed, as we observed from the simulation result in Figure 9B. The increase of suspended sediment concentration will exacerbate the penetration of sun rays, which may deteriorate the photosynthesis event generated by autotroph biota (Wisha *et al.*, 2017).

During neap tidal conditions, the concentration of suspended sediment was not too dramatic. It was ranging from 2-25 mg/L, which equally observed during ebb and flood tide (Figure 9C and 9D). Its relatively higher concentration at the high neap tidal condition tends to spread along the coast, while at the low neap tidal condition, the suspended materials were more scattered. The tidal current was weaker during neap tidal conditions, so that the transport mechanism also tended to deteriorate. It is evident that during neap phases, the semidiurnal tidal component (M2-S2) influence on shallow water will be reduced (Blanton *et al.*, 2002). The current flow tends to be frail, resulting in weakened transport mechanisms within the bay.

Overall, the distribution of suspended materials is higher during spring phases of tidal due to the

more forceful water mass movement and transport mechanism. The current flow oscillating within Sabang Bay twice a day has a profound influence on triggering sediment transport of both sea-sourced sediment and river-sourced materials. The dominant current flow determines the drift of the settled coarse sediment and the turbulence of suspended sediment in the semi-enclosed Sabang Bay.

**CONCLUSION**

Sabang Bay undergoes two-couple tidal oscillations for 24 hours because of its semidiurnal constituent predomination. The periodically changes of tidal elevation control the tidal current, additional waves, and transport mechanism. The vertical sea current profile shows that spiral Ekman induced by Coriolis force occurs during those tidal oscillations with more substantial magnitude in the surface. The current speed is higher during spring phases, followed by the more significant sediment transport in the same condition. The left-ward and right-ward transport seem to be equal, which induces a quite high coarse sediment transport within the bay during high tidal conditions. In contrast, the suspended sediment will be well-scattered during low tidal conditions. The solitary waves from Andaman Sea provenance have a role in inducing higher sand sediment transport, whereby

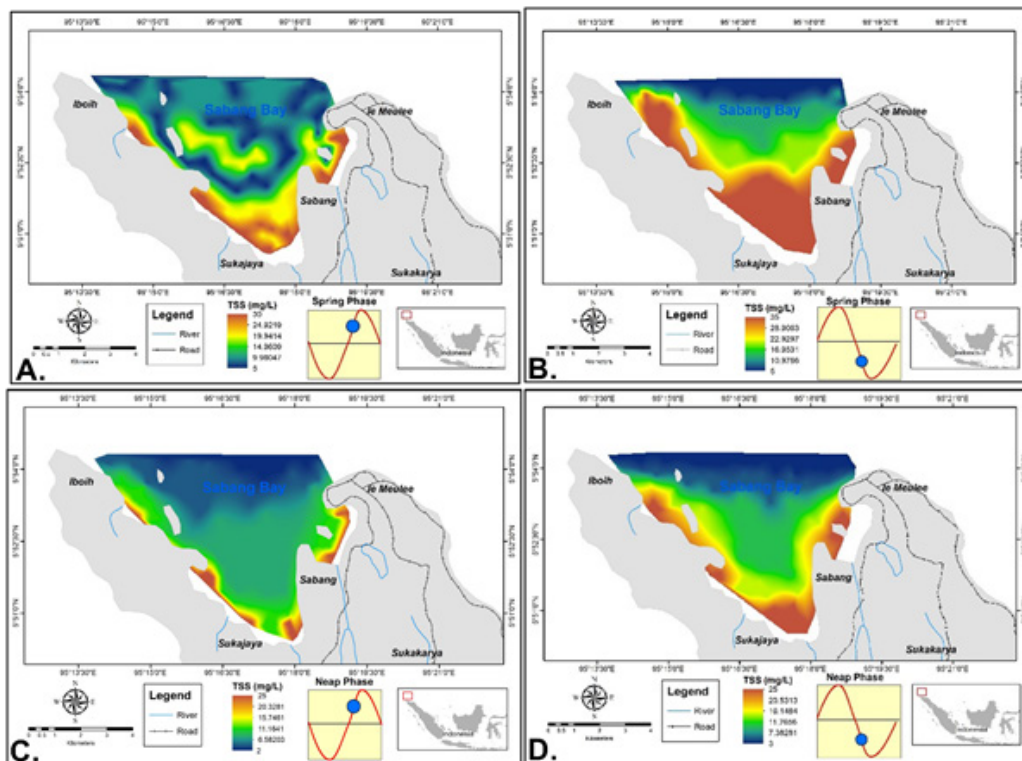


Figure 9. Modeled TSS distribution within Sabang Bay; A. during the high spring tidal condition; B. during the low spring tidal condition; C. during the high neap tidal condition; D. during the low neap tidal condition.

together with the predominance of tidal current, it will cause the higher scour and turbulence within the bay.

## ACKNOWLEDGEMENTS

Acknowledgment and gratitude are given to Research Institute for Coastal Resources and Vulnerability (RICRV) for research funding in Weh Island in 2017, to the Head of RICRV that has a role as research coordinator during the field measurement, and to those who have helped in the completion of this work.

## REFERENCE

- Agus, A. (2019). Analisis Daya Dukung Potensi Wisata Bahari Baru di Kawasan Wisata Pulau Weh Sebagai Pulau Terluar. *PUSAKA (Journal of Tourism, Hospitality, Travel and Business Event)*, 1(2), 1–14. <https://doi.org/10.33649/pusaka.v1i2.14>
- Andutta, F.P., Patterson, R.G., & Wang, X.H. (2019). Monsoon driven waves superpose the effect from macro-tidal currents on sediment resuspension and distribution. *Estuarine, Coastal and Shelf Science*, 223, 85–93. <https://doi.org/10.1016/j.ecss.2019.04.036>
- Bayhaqi, A., Wisha, U.J., & Surinati, D. (2018). Modeling Tidal Current on Banten Bay During Transitional Monsoons. *Jurnal Segara*, 14(2), 95–105. <https://doi.org/10.15578/segara.v14i2.6452>
- Blanton, J. O., Lin, G., & Elston, S. A. (2002). Tidal current asymmetry in shallow estuaries and tidal creeks. *Continental Shelf Research*, 22(11–13), 1731–1743. [https://doi.org/10.1016/S0278-4343\(02\)00035-3](https://doi.org/10.1016/S0278-4343(02)00035-3)
- Boon, J.D. (2013). Secrets of the Tide: Tide and Tidal Current Analysis and Predictions, Storm Surges and Sea Level Trends. In *Elsevier*. <https://doi.org/10.1016/C2013-0-18114-7>
- Chen, J.L., Hsu, T.J., Shi, F., Raubenheimer, B., & Elgar, S. (2015). Hydrodynamic and sediment transport modeling of New River Inlet (NC) under the interaction of tides and waves. *Journal of Geophysical Research: Oceans*, 120(6), 4028–4047. <https://doi.org/10.1002/2014JC010425>
- Chen, W., & de Swart, H.E. (2018). Longitudinal variation in lateral trapping of fine sediment in tidal estuaries: observations and a 3D exploratory model. *Ocean Dynamics*, 68(3), 309–326. <https://doi.org/10.1007/s10236-018-1134-z>
- Fantinato, E. (2019). The impact of (mass) tourism on coastal dune pollination networks. *Biological Conservation*, 236, 70–78. <https://doi.org/10.1016/j.biocon.2019.05.037>
- Gemilang, W.A, Wisha, U.J., Solihuddin, T., Arman, A., & Ondara, K. (2020). Sediment Accumulation Rate in Sayung Coast , Demak , Central Java Using Unsupported. *Atom Indonesia*, 46(1), 25–32. <https://doi.org/https://doi.org/10.17146/aj.2020.935>
- Gemilang, W.A., & Wisha, U.J. (2019). Pengaruh Aktivitas Seafloor Fumaroles Terhadap Sebaran Suhu Permukaan Dan Kondisi Lingkungan Perairan di Teluk Pria Laot, Pulau Weh. *Jurnal Segara*, 15(1), 31–43. <https://doi.org/10.15578/segara.v15i1.6776>
- Gemilang, W.A., Wisha, U.J., & Rahmawan, G.A. (2018). Particle Size Characteristics of Riverbed Sediments Transported by Tidal Bore ‘BONO’ in Kampar Estuary, Riau-Indonesia. *Marine Research in Indonesia*, 43(1), 25–35. <https://doi.org/10.14203/mri.v43i1.293>
- Hunt, S., Bryan, K.R., & Mullarney, J.C. (2015). The influence of wind and waves on the existence of stable intertidal morphology in meso-tidal estuaries. *Geomorphology*, 228, 158–174. <https://doi.org/10.1016/j.geomorph.2014.09.001>
- Kench, P.S., & Mclean, R.F. (2004). Hydrodynamics and sediment flux of Hoa in an Indian Ocean atoll. *Earth Surface Processes and Landforms*, 29(8), 933–953. <https://doi.org/10.1002/esp.1072>
- Menéndez, M., & Woodworth, P.L. (2010). Changes in extreme high water levels based on a quasi-global tide-gauge data set. *Journal of Geophysical Research: Oceans*, 115(C10), 1–15. <https://doi.org/10.1029/2009JC005997>
- Ondara, K., Rahmawan, G.A., Gemilang, W.A., Wisha, U. J., & Dhiauddin, R. (2018). Numerical hydrodynamic wave modelling using spatial discretization in Brebes waters, Central Java, Indonesia. *International Journal on Advanced Science, Engineering and Information Technology*, 8(1). <https://doi.org/10.18517/ijaseit.8.1.4166>
- Ondara, K., Tanto, T.AI., Rahmawan, G.A., Dhiauddin, R., & Wisha, U.J. (2019). Hydro-Oceanographic and Water Quality Assessments As a Basis for the Development of Offshore Aquaculture in the Weh Island , Aceh Province , Indonesia. *Aceh International Journal of Science and Technology*, 8(2), 76–87. <https://doi.org/10.13170/>

aijst.8.2.12362

- Purnawan, S., Ihsan, N., Setiawan, I., & Yuni, S.M. (2018). Tipe sedimen di Perairan Pantai Anoi Itam Kota Sabang. *Depik*, 7(1), 22–27. <https://doi.org/10.13170/depik.7.1.10294>
- Purnawan, S., Alamsyah, T.P.F., Setiawan, I., Rizwan., Ulfah, M., & Rahimi, S.A.El. (2016). Sediment Distribution Analysis in Balohan Bay, Sabang. *Jurnal Ilmu Dan Teknologi Kelautan Tropis*, 8(2), 531–538. <https://doi.org/10.29244/jitkt.v8i2.15812>
- Qarnain, A.G.D., Satriadi, A., & Setiyono, H. (2014). Analysis of Spring and Neap Tides Influence on the sedimentary rate in Timbulsloko Waters, Demak. *Journal of Oceanography*, 3(1), 540–548.
- Rachmat, B., & Purwanto, C. (2016). Morfologi Dasar Laut Kaitannya Dengan Proses Abrasi Pantai Di Perairan Pulau Marore, Sulawesi Utara. *JURNAL GEOLOGI KELAUTAN*, 9(1), 29–43. <https://doi.org/10.32693/jgk.9.1.2011.198>
- Schott, F.A., Xie, S.P., & McCreary, J.P. (2009). Indian ocean circulation and climate variability. *Reviews of Geophysics*, 47(RG1002), 1-46. <https://doi.org/10.1029/2007RG000245>
- Setiawan, I., Rizal, S., Haditjar, Y., Ilhamsyah, Y., Purnawan, S., Irham, M., & Yuni, S. M. (2018). Study of current circulation in the Northern Waters of Aceh. *IOP Conference Series: Earth and Environmental Science*, 12–16. <https://doi.org/10.1088/1755-1315/176/1/012016>
- Stanton, B.R., Goring, D.G., & Bell, R.G. (2001). Observed and modelled tidal currents in the New Zealand region. *New Zealand Journal of Marine and Freshwater Research*, 35(2), 397–415. <https://doi.org/10.1080/00288330.2001.9517010>
- Tanto, T.AI, HR, N.N., & Ilham. (2018). Kualitas Air Laut Untuk Mendukung Wisata Bahari Dan Kehidupan Biota Laut (Studi Kasus: Sekitar Kapal Tenggelam Sophie Rickmers, Perairan Prialaot Sabang). *Jurnal Kelautan: Indonesian Journal of Marine Science and Technology*, 11(2), 173–183. <https://doi.org/10.21107/jk.v11i2.4276>
- Triatmodjo, B. (2012). Perencanaan Bangunan Pantai (2nd ed.). Yogyakarta: Beta Offset Yogyakarta.
- Tsai, C.P., Chen, H. Bin, & Hsu, J.R.C. (2001). Calculations of wave transformation across the surf zone. *Ocean Engineering*, 28(8), 941–955. [https://doi.org/10.1016/S0029-8018\(00\)00047-0](https://doi.org/10.1016/S0029-8018(00)00047-0)
- Van Rijn, L.C. (2011). Analytical and numerical analysis of tides and salinities in estuaries; Part I: Tidal wave propagation in convergent estuaries. *Ocean Dynamics*, 61(11), 1719–1741. <https://doi.org/10.1007/s10236-011-0453-0>
- Wisha, U.J., Dhiauddin, R., & Kusumah, G. (2017). Remote Estimation of Total Suspended Solid (TSS) Transport Affected by Tidal Bore “BONO” of Kampar Big River Estuary Using Landsat 8 OLI Imagery. *Marine Research in Indonesia*, 42(1), 37–45. <https://doi.org/10.14203/mri.v42i1.116>
- Wisha, U.J., Husrin, S., & Prihantono, J. (2015). Hidrodinamika Perairan Teluk Banten Pada Musim Peralihan (Agustus–September). *ILMU KELAUTAN: Indonesian Journal of Marine Sciences*, 20(2), 101–112. <https://doi.org/10.14710/ik.ijms.20.2.101-112>
- Wisha, U.J., Ondara, K., & Kusumah, G. (2017). An Overview of Surface Water Quality Influenced by Suspended Solid Content in the Sayung Waters, Demak, Indonesia. *Jurnal Segara*, 13(2), 107–117. <https://doi.org/https://doi.org/10.15578/segara.v13i2.6446>
- Wisha, U.J., Rahmawan, G.A., Ondara, K., Gemilang, W.A., Dhiauddin, R., Ridwan, N.N.H., & Ilham. (2019). Offshore Floating Marine Fish Cage Aquaculture Development Planning Evaluation Based on Hydro-Oceanography Conditions in Sabang Bay, Weh Island. *Jurnal Ilmu Dan Teknologi Kelautan Tropis*, 11(1), 151–162. <https://doi.org/10.29244/jitkt.v11i1.24780>